SHAPE OPTIMIZATION USING THE BEM AND SAND FORMULATIONS

Alfredo Canelas, acanelas@fing.edu.uy
José Herskovits, jose@optimize.ufrj.br
COPPE - Federal University of Rio de Janeiro, Mechanical Engineering Program. Post office box 68503, CEP 21945 970, Rio de Janeiro-RJ, Brazil.

José Claudio de Faria Telles, telles@coc.ufrj.br
COPPE - Federal University of Rio de Janeiro, Civil Engineering Program.

Abstract. *The shape optimization problem consists of looking for the geometry that minimizes an objective function, like mass or compliance, subject to mechanical constraints. The Boundary Element Method (BEM) is used for the structural analysis. For linear elasticity problems, it needs only a mesh on the boundary of the structure. This characteristic makes the BEM a natural method for shape optimization, since only the boundary is needed to define the optimization problem and to carry out the structural analysis. The Simultaneous Analysis and Design formulation (SAND) is used here to define the shape optimization problem. It considers the state variables as unknowns of the optimization problem and includes the equilibrium equations as equality constraints. In this way, it is not necessary to solve the equilibrium equation per iteration; the equilibrium is only obtained at the end of the optimization process.*
Three different models for shape optimization are studied. The first one minimizes the compliance of the structure subject to a constraint on the volume. The second one minimizes the maximal von Mises stress on the boundary. The third model looks for a full stress design minimizing the mean value on the boundary of the square of the von Mises stress minus a reference value.
The optimization problems are solved employing a feasible interior point method for nonlinear programming. Here, the discrete sensitivity analysis is used to compute first and second derivatives of the functions arising in the formulations.
Numerical results for several two-dimensional linear elasticity examples are presented. A comparison among the three models is done for the presented examples.

Keywords: *Shape optimization, Boundary Element Method, Interior Point Algorithm*

1. INTRODUCTION

The shape optimization problem consists of looking for the geometry that minimizes an objective function, like mass or compliance, subject to mechanical constraints. It is a traditional field in Structural Design, and there are many books and surveys dealing with it and related fields (Sokolowski and Zolesio, 1992; Bendsøe, 1995; Choi and Kim, 2004; Kwak, 1994; van Keulen et al., 2005; Haftka and Grandhi, 1986; Pedersen, 2000).

The Boundary Element Method (BEM) is a widely employed numerical method for structural analysis (Brebbia et al., 1984; París and Cañas, 1998; Beer and Watson, 1992; Brebbia and Dominguez, 1992). It is based on an integral form of the equilibrium equations. For linear elasticity problems the BEM just needs a mesh for the boundary of the structure. The state variables are the nodal displacements and stresses in this boundary. This feature makes the BEM a natural method for shape optimization since the discretization on the boundary is enough to define the optimization problem and to perform the structural analysis. For this reason, the BEM has been widely studied for applications in Shape Optimization (Parvizian and Fenner, 1997; Tafreshi, 2002; Burczyński, 1993; Wessel et al., 2004; Cerrolaza et al., 2000; Bialecki et al., 2005; Kita and Tanie, 1997; Barra, 1990; Martin and Dulikravich, 2004; Sfantos and Aliabadi, 2006; Meric, 1995).

The Simultaneous Analysis and Design formulation (SAND) is frequently used in structural design (Haftka, 1985; Haftka and Kamat, 1989; Wang and Arora, 2004; Herskovits et al., 2005). It considers the state variables of the structural model as unknowns for the optimization problem and includes the equilibrium equations as equality constraints. One of the difficulties when using the SAND formulation is due to the large increase in the number of variables and constraints of the optimization problem. Luckily, it generally turns easily the computation of function derivatives and several methods for large applications have been presented. In references (Haftka, 1985; Haftka and Kamat, 1989; Wang and Arora, 2004; Herskovits et al., 2005) the SAND formulation that uses the Finite Element Method (FEM) is studied. In that situation, the sparsity of the functions arising in the SAND formulation is of main importance, then, optimization algorithms that uses effectively such property allows the optimization be possible in large applications. In reference (Herskovits et al., 2005) an optimization algorithm for SAND formulation is proposed and used effectively to solve some examples, it also has the advantage of being able to use existent codes for the analysis and computation of derivatives.

When the BEM is used for the structural analysis, an important reduction in the number of state variables is obtained when compared with the FEM. Unfortunately, the matrices of derivatives of the functions arising in the formulation are not sparse any more. Furthermore, in large applications there are still a large number of state variables. Then, the optimization algorithm to be used with this SAND formulation should ideally be efficient for such large scale problems.

Recent works indicate Primal-Dual interior point algorithms as well-suited to solve large scale optimization problems (Benson et al., 2001; Morales et al., 2002; Dolan and Moré, 2004). As pointed out in these references, this kind of algorithms reduce significantly the computer run time. Unfortunately, these algorithms need second derivatives which are generally too expensive in shape optimization. Consequently, most of the works using the BEM does not make use of the SAND formulation and employ algorithms that use, at most, first derivatives (Parvizian and Fenner, 1997; Tafreshi, 2002; Burczyński, 1993; Wessel et al., 2004; Cerrolaza et al., 2000; Bialecki et al., 2005; Kita and Tanie, 1997) and, sometimes, algorithms which do not employ any sensitivity information as in references (Wessel et al., 2004; Cerrolaza et al., 2000; Bialecki et al., 2005; Kita and Tanie, 1997). Because of that, most of the works dealing with sensitivity analysis using BEM discuss the numerical computation of first derivatives only (Burczyński, 1993; Barra, 1990; Martin and Dulikravich, 2004; Sfantos and Aliabadi, 2006; Meric, 1995).

In (Canelas et al., 2007) the authors took advantage of the partial separability property of the functions arising in the SAND formulation that is still present when using the BEM. This property makes possible to define routines which compute the first and second derivatives (and next order derivatives too) with the same complexity in terms of number of basic operations as the complexity of computing the functions themselves. In (Canelas et al., 2007) it is shown that the mass, equilibrium and compliance are described by function which satisfy the partial separability property. That is also true for the von Mises stresses present on the boundary and is shown later on this paper.

The method for shape optimization presented in (Canelas et al., 2007), which is based on the SAND formulation and uses the BEM for the analysis and a feasible primal-dual interior point algorithm for the solution of the optimization problem, is employed here. This paper extends the results obtained in (Canelas et al., 2007) considering shape optimization models that take into account the von Mises stresses on the boundary of the structure.

Numerical results for several two-dimensional linear elasticity examples are studied. A comparison among three employed models for shape optimization is presented.

2. BOUNDARY ELEMENT METHOD

The linear elasticity problem in two dimensions consists in finding the functions $\mathbf{u}$ and $\boldsymbol{\sigma}$ that define the displacements and stresses, respectively, on points of the domain of an elastic solid Ω included in the two-dimensional Euclidean space. The boundary conditions are given by the functions $\bar{\mathbf{u}}$ and $\bar{\mathbf{p}}$ defined over complementary regions on the boundary Γ of Ω (see Fig. 1).

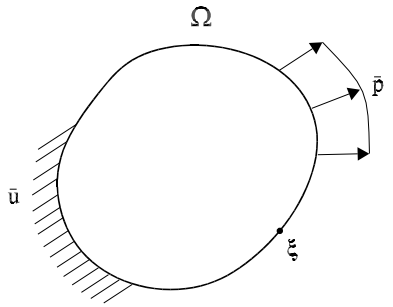

Figure 1. Linear elasticity problem.

The Boundary Element Method (BEM) is based on an integral equation that is known as Somigliana's identity for the displacements. For null body forces, it can be written in matrix form as:

$$\mathbf{c}(\boldsymbol{\xi})\mathbf{u}(\boldsymbol{\xi}) = \int_\Gamma \mathbf{u}^*(\boldsymbol{\xi},\mathbf{x})\mathbf{p}(\mathbf{x})\,\mathrm{d}\Gamma - \int_\Gamma \mathbf{p}^*(\boldsymbol{\xi},\mathbf{x})\mathbf{u}(\mathbf{x})\,\mathrm{d}\Gamma \tag{1}$$

Here, the source point $\boldsymbol{\xi}$ will be taken on the boundary Γ. The matrix $\mathbf{c}$ is a function of the boundary geometry at the point $\boldsymbol{\xi}$ and the second integral on the right in Eq. (1) must be calculated in the Cauchy principal value sense.

The function $\mathbf{u}^*$ represents the fundamental solution for the linear elasticity problem, the function $\mathbf{p}^*$ is its corresponding surface stress or traction. For plane strain the fundamental displacements and tractions, in index notation, are given by:

$$\mathbf{u}^*_{ij}(\boldsymbol{\xi},\mathbf{x}) = \frac{-1}{8\pi(1-\nu)G}\left\{(3-4\nu)\log(r)\delta_{ij} - r_{,i}r_{,j}\right\} \tag{2}$$

$$\mathbf{p}^*_{ij}(\boldsymbol{\xi},\mathbf{x}) = \frac{-1}{4\pi(1-\nu)r}\left\{\left[(1-\nu)\delta_{ij} + 2r_{,i}r_{,j}\right]\frac{\partial r}{\partial n} - (1-\nu)(r_{,i}\mathbf{n}_j - r_{,j}\mathbf{n}_i)\right\} \tag{3}$$

where $r = r(\boldsymbol{\xi}, \mathbf{x})$ is the distance between the source point $\boldsymbol{\xi}$ and the field point $\mathbf{x}$, $r = \|\mathbf{x} - \boldsymbol{\xi}\|$, and the derivatives $r_{,i} = \partial r / \partial x_i$. G and ν are the shear modulus and the Poisson's ratio, respectively, of the elastic material and $\mathbf{n}$ is the outward normal vector to Γ at the point $\mathbf{x}$. For plane stress the Poisson's ratio v must be replaced by $\bar{\nu} = \nu/(1+\nu)$.

The BEM discretization consists in dividing the boundary Γ in a set of elements $\Gamma^{(j)}$, $1 \leq j \leq n_e$. The geometry and the functions $\mathbf{u}$ and $\mathbf{p}$ are defined through interpolation of the nodal values. In the following, $\boldsymbol{\xi}^i$, $\mathbf{u}^i$ and $\mathbf{p}^i$ will denote the position, displacement and traction at node i, $\boldsymbol{\xi}^{(j)}$, $\mathbf{u}^{(j)}$ and $\mathbf{p}^{(j)}$ will denote the vectors of nodal values for the element j. For linear elements, the functions in $\Gamma^{(j)}$ are given by:

$$\begin{array}{rcl} \boldsymbol{\xi}(\eta) & = & \boldsymbol{\Phi}(\eta)\boldsymbol{\xi}^{(j)} \\ \mathbf{u}(\eta) & = & \boldsymbol{\Phi}(\eta)\mathbf{u}^{(j)} \\ \mathbf{p}(\eta) & = & \boldsymbol{\Phi}(\eta)\mathbf{p}^{(j)} \end{array} ; \quad \boldsymbol{\Phi}(\eta) = \begin{pmatrix} \phi_1(\eta) & 0 & \phi_2(\eta) & 0 \\ 0 & \phi_1(\eta) & 0 & \phi_2(\eta) \end{pmatrix}; \quad \begin{array}{rl} \phi_1(\eta) & = (1/2)(1-\eta) \\ \phi_2(\eta) & = (1/2)(1+\eta) \end{array} \tag{4}$$

Applying Eq. (1) to the node $\boldsymbol{\xi}^i$ and assuming the boundary was divided in n_e elements, the resulting equation is:

$$\mathbf{c}(\boldsymbol{\xi}^i)\mathbf{u}^i = \sum_{j=1}^{n_e} \left\{ \int_{\Gamma^{(j)}} \mathbf{u}^*(\boldsymbol{\xi}^i, \mathbf{x}) \boldsymbol{\Phi} \mathbf{p}^{(j)} \, \mathrm{d}\Gamma \right\} - \sum_{j=1}^{n_e} \left\{ \int_{\Gamma^{(j)}} \mathbf{p}^*(\boldsymbol{\xi}^i, \mathbf{x}) \boldsymbol{\Phi} \mathbf{u}^{(j)} \, \mathrm{d}\Gamma \right\} \tag{5}$$

The element matrices are defined by:

$$\hat{\mathbf{h}}_{ij} = \int_{\Gamma^{(j)}} \mathbf{p}^*(\boldsymbol{\xi}^i, \mathbf{x}) \boldsymbol{\Phi} \, \mathrm{d}\Gamma; \qquad \mathbf{g}_{ij} = \int_{\Gamma^{(j)}} \mathbf{u}^*(\boldsymbol{\xi}^i, \mathbf{x}) \boldsymbol{\Phi} \, \mathrm{d}\Gamma \tag{6}$$

With these definitions, Eq. (5) can be written as:

$$\mathbf{c}(\boldsymbol{\xi}^i)\mathbf{u}^i + \sum_{j=1}^{n_e} \hat{\mathbf{h}}_{ij} \mathbf{u}^{(j)} - \sum_{j=1}^{n_e} \mathbf{g}_{ij} \mathbf{p}^{(j)} = 0 \tag{7}$$

The first term can be summed to the second one to obtain:

$$\sum_{j=1}^{n_e} \mathbf{h}_{ij} \mathbf{u}^{(j)} - \sum_{j=1}^{n_e} \mathbf{g}_{ij} \mathbf{p}^{(j)} = 0 \tag{8}$$

where $\mathbf{h}_{ij}$ was defined implicitly. Applying Eq. (8) to all the nodes, it results in the BEM system of equations which can be written as:

$$\mathbf{H}(\boldsymbol{\xi})\mathbf{u} - \mathbf{G}(\boldsymbol{\xi})\mathbf{p} = 0 \tag{9}$$

where the vectors $\boldsymbol{\xi}$, $\mathbf{u}$ and $\mathbf{p}$ define the position, displacement and tractions on all the nodes of the boundary.

2.1 Stresses on the boundary

Here, the stresses are evaluated only on the boundary of the structure. That can be done expressing displacements and tractions on the element in local coordinates and employing Hooke's law for determining the components of the stress tensor. Employing the local coordinates shown by Fig. 2, the strain component $\bar{\boldsymbol{\epsilon}}_{11}$ can be obtained as (Brebbia et al., 1984):

$$\bar{\boldsymbol{\epsilon}}_{11} = \frac{\partial \bar{\mathbf{u}}_1}{\partial \bar{\mathbf{x}}_1} \tag{10}$$

where, the derivative is applied to Eq. (4) that define the displacements on the boundary. For plane strain problems the required three components of the stress tensor are given by (Brebbia et al., 1984):

$$\bar{\boldsymbol{\sigma}}_{11} = \frac{1}{1-\nu}(\nu \bar{\boldsymbol{\sigma}}_{22} + 2G\bar{\boldsymbol{\epsilon}}_{11}); \qquad \bar{\boldsymbol{\sigma}}_{12} = \bar{\mathbf{p}}_1; \qquad \bar{\boldsymbol{\sigma}}_{22} = \bar{\mathbf{p}}_2 \tag{11}$$

The same formulas are valid for plane stress if ν is replaced by $\bar{\nu}$.

The von Mises stress σ^M on the element can be calculated employing Eq. (12) where the component $\bar{\boldsymbol{\sigma}}_{33}$ must be taken $\bar{\boldsymbol{\sigma}}_{33} = \nu(\bar{\boldsymbol{\sigma}}_{11} + \bar{\boldsymbol{\sigma}}_{22})$ for plane strain and zero for the case of plane stress.

$$\sigma^M = \sqrt{\bar{\boldsymbol{\sigma}}_{11}^2 + \bar{\boldsymbol{\sigma}}_{22}^2 + \bar{\boldsymbol{\sigma}}_{33}^2 - \bar{\boldsymbol{\sigma}}_{11}\bar{\boldsymbol{\sigma}}_{22} - \bar{\boldsymbol{\sigma}}_{11}\bar{\boldsymbol{\sigma}}_{33} - \bar{\boldsymbol{\sigma}}_{22}\bar{\boldsymbol{\sigma}}_{33} + 3\bar{\boldsymbol{\sigma}}_{12}} \tag{12}$$

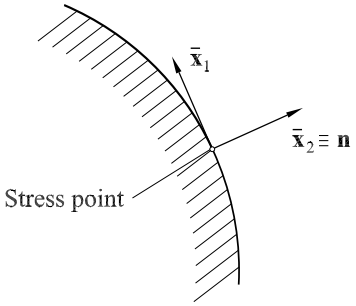

Figure 2. Local coordinate system at the stress point.

3. THREE MODELS FOR SHAPE OPTIMIZATION

3.1 Model 1 - Compliance optimization

The first model considered here is the largely employed model in topology optimization that consists in minimizing the compliance of the structure subject to a constraint in the volume. The following optimization problem is solved:

$$\begin{array}{lll} \text{minimize} & c(\mathbf{u},\mathbf{p}) & \\ \text{subject to:} & \mathbf{h}(\boldsymbol{\xi}(\mathbf{q}),\mathbf{u},\mathbf{p})=0 & \\ & \mathbf{u}_i=\bar{\mathbf{u}}_i & i\in I_{\mathbf{u}} \\ & \mathbf{p}_i=\bar{\mathbf{p}}_i & i\in I_{\mathbf{p}} \\ & v(\boldsymbol{\xi}(\mathbf{q}))\leq v_0 & \end{array} \tag{13}$$

Here, $\mathbf{q}$ is the vector of the variables that define the geometry of the boundary. In order to define its geometry, the well known B-Spline curves are used (Samareh, 1999; Braibant and Fleury, 1984), these curves are represented in Eq. (13) by the linear function $\boldsymbol{\xi}(\mathbf{q})$ that gives the nodal coordinates of a mesh with respect to the spline parameters $\mathbf{q}$. Vectors $\mathbf{u}$ and $\mathbf{p}$ define the displacements and stresses on the boundary. The compliance function c can be defined as: $c(\mathbf{u},\mathbf{p})=\int_\Gamma \mathbf{u}(\mathbf{x})^T\mathbf{p}(\mathbf{x})\,\mathrm{d}\Gamma$. The function v represents the volume of the body which must be less than the positive parameter v_0. Function $\mathbf{h}$ is defined as: $\mathbf{h}(\boldsymbol{\xi}(\mathbf{q}),\mathbf{u},\mathbf{p})=\mathbf{H}(\boldsymbol{\xi}(\mathbf{q}))\mathbf{u}-\mathbf{G}(\boldsymbol{\xi}(\mathbf{q}))\mathbf{p}$. This function represents the equilibrium and compatibility equations derived from the integral equation described in Section 2. Vectors $\bar{\mathbf{u}}$ and $\bar{\mathbf{p}}$ and the sets of indices $I_{\mathbf{u}}$ and $I_{\mathbf{p}}$ define the boundary conditions for the elasticity problem.

In reference (Canelas et al., 2007) the partial separability property for the performance functions c, $\mathbf{h}$, and v was proven. This property makes possible to code very efficient procedures for the computation of the function derivatives required by the optimization algorithm.

3.2 Model 2 - Minimization of the maximal von Mises stress

This model consists in minimizing the maximal von Mises stress on the boundary of the structure considering a constraint in the total volume. In order to avoid non-differentiable functions, an auxiliary variable z is employed and the problem is formulated as:

$$\begin{array}{lll} \text{minimize} & z & \\ \text{subject to:} & \mathbf{h}(\boldsymbol{\xi}(\mathbf{q}),\mathbf{u},\mathbf{p})=0 & \\ & \mathbf{u}_i=\bar{\mathbf{u}}_i & i\in I_{\mathbf{u}} \\ & \mathbf{p}_i=\bar{\mathbf{p}}_i & i\in I_{\mathbf{p}} \\ & z\geq \sigma_j^M(\mathbf{u},\mathbf{p}) & j\in I_M \\ & v(\boldsymbol{\xi}(\mathbf{q}))\leq v_0 & \end{array} \tag{14}$$

where σ_j^M represent the von Mises stress at element j which, in this SAND formulation, depends on vectors $\mathbf{u}$ and $\mathbf{p}$ only. The set I_M is the set of points where the von Mises stress is considered. It is defined as a subset of the nodes of the employed mesh (It can contain all the nodes of the mesh).

As shown by Section 2, the von Mises stresses on element j depend only on the variables related to this element, then, each inequality constraint considering the von Mises stress depends on variables $\boldsymbol{\xi}^{(j)}$, $\mathbf{u}^{(j)}$, $\mathbf{p}^{(j)}$ and z. Then, the partial separability property of these constraints is straightforward.

3.3 Model 3 - Mean value optimization of the von Mises stress

This model consists in minimizing the integral of the square of the difference of the actual von Mises stress and a reference value as proposed by Herskovits et al. (1996). It also considers a constraint in the volume. Then, the shape optimization problem can be expressed as:

$$\begin{array}{lll} \text{minimize} & f(\boldsymbol{\xi}(\mathbf{q}),\mathbf{u},\mathbf{p}) = \int_\Gamma (\sigma^M(\mathbf{x}) - \sigma^R)^2 \,\mathrm{d}\Gamma & \\ \text{subject to:} & \mathbf{h}(\boldsymbol{\xi}(\mathbf{q}),\mathbf{u},\mathbf{p}) = 0 & \\ & \mathbf{u}_i = \bar{\mathbf{u}}_i \qquad\quad i \in I_{\mathbf{u}} & \\ & \mathbf{p}_i = \bar{\mathbf{p}}_i \qquad\quad i \in I_{\mathbf{p}} & \\ & v(\boldsymbol{\xi}(\mathbf{q})) \leq v_0 & \end{array} \tag{15}$$

In Eq. (15) the function f depends on variable $\mathbf{q}$ through the domain Γ of integration, and σ^R is a reference value defined a priori. It can be an admissible value of the von Mises stress for the employed material.

Function f has also the partial separability property. This can easily seen expressing f as a sum of n_e integrals over the elements. Each integral depends only on variables $\boldsymbol{\xi}^{(j)}$, $\mathbf{u}^{(j)}$ and $\mathbf{p}^{(j)}$.

4. EXAMPLES

This section presents results for three examples of plane stress shape optimization problems. The three described models were employed for each example. The feasible interior point algorithm for nonlinear optimization described in (Canelas et al., 2007) was employed here for finding the optimal solution. A linear elastic material with Young's modulus $E = 1.0$ N/m^2 and Poisson's ratio $\nu = 0.3$ was used in all the examples.

The first example consists of looking for the optimal shape of a hole in a plate as is depicted by Fig. 3. The measures of Fig. 3 as the ones of Figs. 5 and 9 are in meters. The values of the applied tractions are: $\mathrm{P}_1 = 1.5$ N/m and $\mathrm{P}_2 = 1.0$ N/m. The three models for shape optimization give, in this case, similar results. Figure 4 shows the von Mises stresses obtained with Model 1 for one quarter of the plate. The second example is shown by Fig. 5. There, the fillet that is looked for is drawn in dashed lines. The entire fillet must be located between the vertical dash-dot lines. The value of the applied traction is $\mathrm{P} = 1.0$ N/m. The obtained results are shown for a half of the fillet by Figs. 6, 7 and 8 for the three employed models. The third example is depicted by Fig. 9. In this example the geometry of a plane frame is looked for. Points A, B, C and D of Fig. 9 are fixed and points E and F can move horizontally. The obtained results are shown for a half of the frame by Figs. 10, 11 and 12.

The parameters of the models and the results of the final area of the structure and maximal value of the von Mises stress are shown by Table 1. The reference value σ^R of Model 3 was chosen equal to 3.0 N/m^2 for the plate which is an intermediate value between the maximal von Mises stresses obtained for models 1 and 2. For the fillet and the frame it was chosen equal to the applied tractions.

The main conclusions about the results are: 1) Model 1 worked well for the plate but presented solutions with high von Mises stresses for the fillet and the frame. That seems to be due to the constraints imposed to the optimal shape: the fillet has to be between the vertical dash-dot lines of Fig. 5 and the frame has points A and B of Fig. 9 fixed. This model always made use of all the available material as is shown by Table 1 and put the material where the higher stresses were. That reduces the compliance for these examples but is not the best strategy for reducing the von Mises stresses. For example, Model 2 did not employ all the available material for the fillet, i.e., the area constraint is not active at the solution. For the frame, Model 1 put the material around point A of Fig. 9, that reduces the compliance significantly but at the same time increases the von Mises stress at this point. The best strategy for this example, followed by Model 2, is to put the material on the opposite side, i.e., around point E of Fig. 9 where the smaller von Mises stresses are. That reduces the stresses effectively around point A. 2) Model 2 presented the best solutions for all the examples in terms of maximal von Mises stress. The main disadvantage of this model is that it is much more time consuming than the other models. That is mainly due to the large number of inequality constraints related to the von Mises stresses. 3) Model 3 worked better than Model 1, it presented good solutions for all the examples. Compared with Model 2 it presented higher maximal von Mises stresses because it did not reduce the stress concentration completely on the right of the fillet and did not make use of all the material in the case of the frame. However, it could find these relatively good solutions being much less time consuming than Model 2.

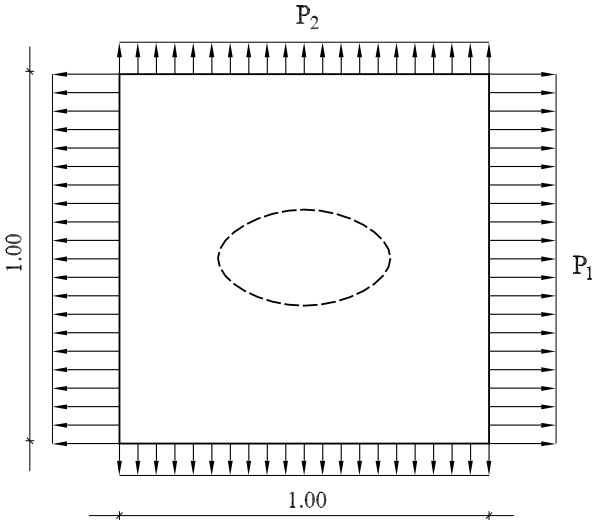

Figure 3. Optimization of a plate with a hole.

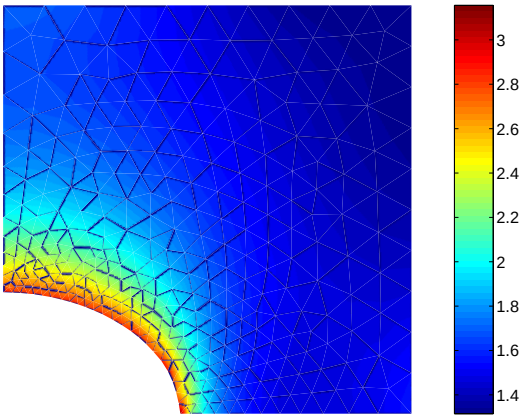

Figure 4. Von Mises stresses in the plate - Model 1.

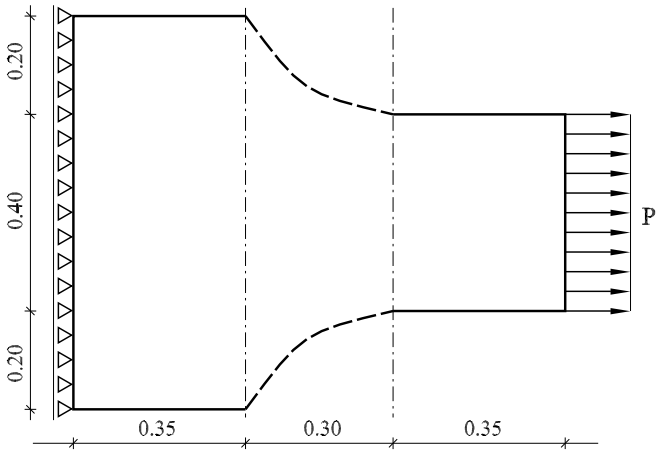

Figure 5. Optimization of a Fillet.

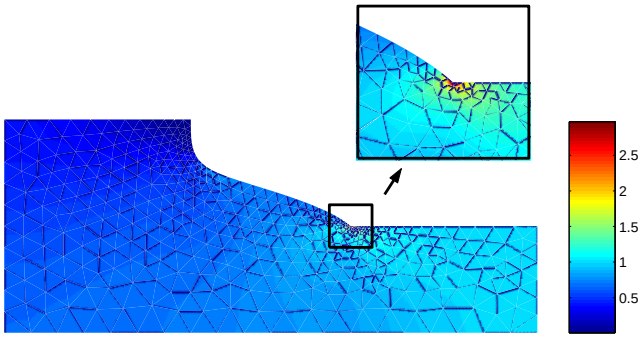

Figure 6. Von Mises stresses in the fillet - Model 1.

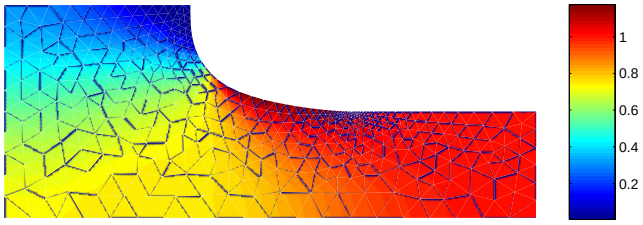

Figure 7. Von Mises stresses in the fillet - Model 2.

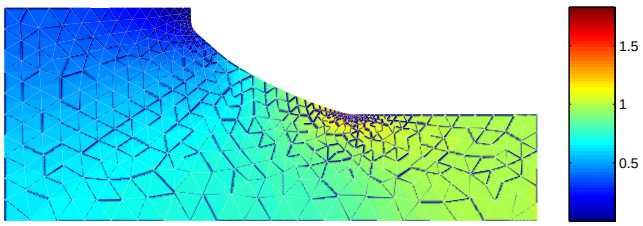

Figure 8. Von Mises stresses in the fillet - Model 3.

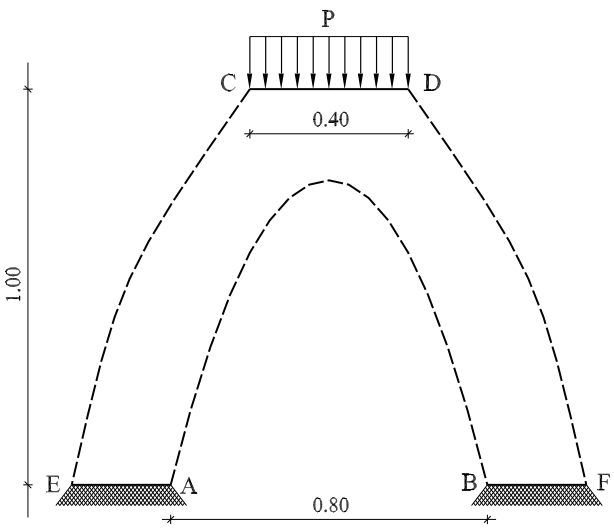

Figure 9. Optimization of a plane frame.

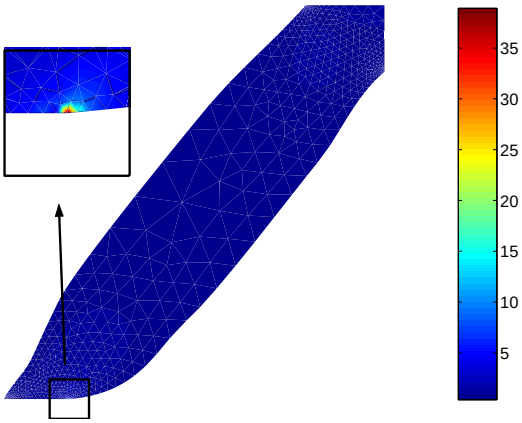

Figure 10. Von Mises stresses in the frame - Model 1.

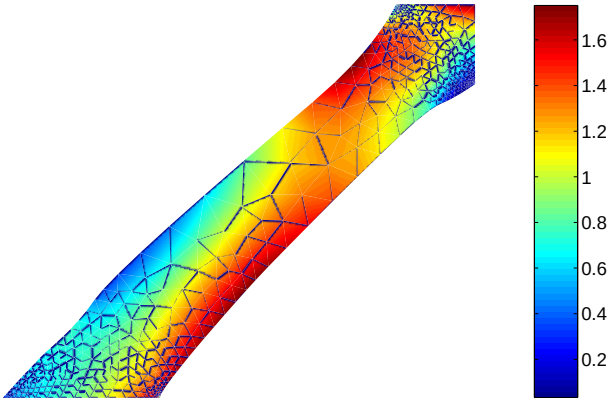

Figure 11. Von Mises stresses in the frame - Model 2.

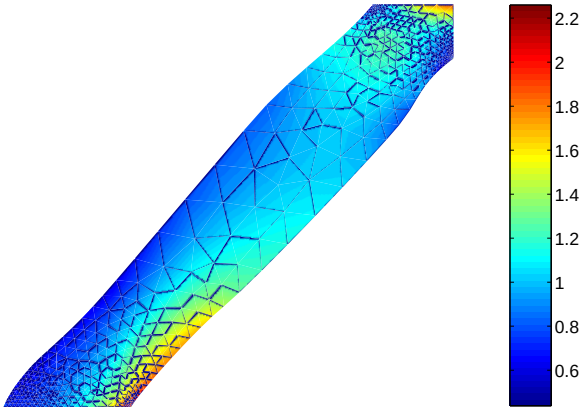

Figure 12. Von Mises stresses in the frame - Model 3.

Table 1. Parameters and obtained values for the presented examples.

Example	v_0 (m^2)	σ^R (N/m^2)	Final area (m^2)	σ^M_{max} (N/m^2)
Plate - Model 1	3.60	-	3.600	3.16
Plate - Model 2	3.60	-	3.600	2.83
Plate - Model 3	3.60	3.0	3.427	3.02
Fillet - Model 1	0.58	-	0.580	2.97
Fillet - Model 2	0.58	-	0.559	1.15
Fillet - Model 3	0.58	1.0	0.578	1.83
Frame - Model 1	0.70	-	0.700	38.92
Frame - Model 2	0.70	-	0.700	1.70
Frame - Model 3	0.70	1.0	0.671	2.26

5. CONCLUSIONS

This work extend the application of the shape optimization method proposed in (Canelas et al., 2007) to models considering performance functions related to the von Mises stresses present on the boundary of the structure. In particular, it was shown that these performance functions have the partial separability property required for efficient evaluation of the function derivatives. Three models for shape optimization were tested: Model 1 minimizes the compliance of the structure subject to a constraint on the volume, Model 2 minimizes the maximal von Mises stress on the boundary and Model 3 minimizes the mean value on the boundary of the square of the von Mises stress minus a reference value. It was shown that Model 1 can present solutions with high von Mises stresses if constraints on the shape are imposed. Model 2 presented the best results in terms of the maximal von Mises stress but is, unfortunately, much more time consuming than the other models. Model 3 presented relatively good solutions for the studied examples being much less time consuming than Model 2.

6. REFERENCES

Barra, L. P. (1990), Sensitivity analysis - an application of the boundary element method to shape optimization (in Portuguese), Master's thesis, Federal University of Rio de Janeiro, COPPE, Rio de Janeiro, Brazil.

Beer, G. and Watson, J. O. (1992), *Introduction to Finite and Boundary Element Methods for Engineers*, Wiley.

Bendsøe, M. P. (1995), *Optimization of structural topology, shape and material*, Springer, Berlin, Heidelberg, New York.

Benson, H. Y., Shanno, D. F. and Vanderbei, R. J. (2001), A comparative study of large-scale nonlinear optimization algorithms, Technical Report ORFE 01-04, Department of Operations Research and Financial Engineering, Princeton University, Princeton, NJ 08544.

Bialecki, R. A., Burczynski, T., Dlugosz, A., Kus, W. and Ostrowski, Z. (2005), 'Evolutionary shape optimization of thermoelastic bodies exchanging heat by convection and radiation', *Computer Methods in Applied Mechanics and Engineering* **194**, 1839–1859.

Braibant, V. and Fleury, C. (1984), 'Shape optimal design using B-Splines', *Computer Methods in Applied Mechanics and Engineering* **44**, 247–267.

Brebbia, C. A. and Dominguez, J. (1992), *Boundary Elements - An Introductory Course*, 2nd edn, Mc-Graw-Hill.

Brebbia, C. A., Telles, J. C. F. and Wrobel, L. C. (1984), *Boundary Element Technique: Theory and Applications in Engineering*, Springer - Verlag.

Burczyński, T. (1993), 'Applications of BEM in sensitivity analysis and optimization', *Computational Mechanics* **13**, 29–44.

Canelas, A., Herskovits, J. and Telles, J. C. F. (2007), Shape optimization using the boundary element method and a SAND interior point algorithm for constrained optimization. Accepted for publication in Computers & Structures.

Cerrolaza, M., Annicchiarico, W. and Martinez, M. (2000), 'Optimization of 2D boundary element models using β-splines and genetic algorithms', *Engineering Analysis with Boundary Elements* **24**, 427–440.

Choi, K. K. and Kim, N. H. (2004), *Structural Sensitivity Analysis and Optimization, 1 and 2*, Springer, Berlin, Heidelberg, New York.

Dolan, E. D. and Moré, J. J. (2004), Benchmarking optimization software with COPS 3.3, Technical Report ANL/MCS-TM-273, Argonne National Laboratory, Argonne, Illinois, USA.

Haftka, R. T. (1985), 'Simultaneous analysis and design', *AIAA Journal* **23**, 1099–1103.

Haftka, R. T. and Grandhi, R. V. (1986), 'Structural shape optimization - a survey', *Comput. Methods Appl. Mech. Eng.* **57**, 91–106.

Haftka, R. T. and Kamat, M. P. (1989), 'Simultaneous nonlinear structural analysis and design', *Comput. Mech.* **4**, 409–416.

Herskovits, J., Dias, G. P. and Mota Soares, C. (1996), 'A full stress technique for structural shape optimization', *Applied Mathematics and Computer Science* **6**(2), 303–319.

Herskovits, J., Mappa, P., Goulart, E. and Mota Soares, C. M. (2005), 'Mathematical programming models and algorithms for engineering design optimization', *Computer Methods in Applied Mechanics and Engineering* **194**, 3244–3268.

Kita, E. and Tanie, H. (1997), 'Shape optimization of continuum structures by genetic algorithm and boundary element method', *Engineering Analysis with Boundary Elements* **19**, 129–136.

Kwak, B. M. (1994), 'A review on shape optimal design and sensitivity analysis', *Struct. Eng. / Earthq. Eng.* **10**(4), 159–174.

Martin, T. J. and Dulikravich, G. S. (2004), 'An implicit and explicit BEM sensitivity approach for thermo-structural optimization', *Engineering Analysis with Boundary Elements* **28**, 257–265.

Meric, R. A. (1995), 'Differential and integral sensitivity formulations and shape optimization by BEM', *Engineering Analysis with Boundary Elements* **15**, 181–188.

Morales, J. L., Nocedal, J., Waltz, R. A., Liu, G. and Goux, J. P. (2002), Assessing the potential of interior methods for nonlinear optimization, *in* O. Ghattas, ed., 'Proceedings of the First Sandia Workshop on Large-Scale PDE-Constrained Optimization', Springler Verlag, Heidelberg, Berlin, New York.

París, F. and Cañas, J. (1998), *Boundary Element Method - Fundamentals and Applications*, Oxford University Press.

Parvizian, J. and Fenner, R. T. (1997), 'Shape optimization by the boundary element method: a comparison between mathematical programming and normal movement approaches', *Engineering Analysis with Boundary Elements* **19**, 137–145.

Pedersen, P. (2000), 'On optimal shapes in materials and structures', *J. Theor. Appl. Mech.* **19**, 169–182.

Samareh, J. A. (1999), A survey of shape parameterization techniques, Technical Report NASA-CP-1999-209136, NASA Langley Research Center, Hampton, VA 23681.

Sfantos, G. K. and Aliabadi, M. H. (2006), 'A boundary element sensitivity formulation for contact problems using the implicit differentiation method', *Engineering Analysis with Boundary Elements* **30**(1), 22–30.

Sokolowski, J. and Zolesio, J. P. (1992), *Introduction to Shape Optimization - Shape Sensitivity Analysis*, Springer-Verlag, Berlin, Heidelberg, New York.

Tafreshi, A. (2002), 'Shape design sensitivity analysis of 2D anisotropic structures using the boundary element method', *Engineering Analysis with Boundary Elements* **26**, 237–251.

van Keulen, F., Haftka, R. T. and Kim, N. H. (2005), 'Review of options for structural design sensitivity analysis. Part 1: linear systems', *Comput. Methods Appl. Mech. Eng.* **194**, 3213–3243.

Wang, Q. and Arora, J. S. (2004), Optimization of large-scale structural systems using sparse SAND formulations, Technical report, Optimal Design Lab/CCAD, College of Engineering/4110 SC, The University of Iowa, Iowa City, IA 52242.

Wessel, C., Cisilino, A. and Sensale, B. (2004), 'Structural shape optimisation using boundary elements and the biological growth method', *Struct. Multidisc. Optim.* **28**, 221–227.

7. Responsibility notice

The author(s) is (are) the only responsible for the printed material included in this paper.